The role of Microgrid controller to increase the profitability for both owner and distribution network operator

1st Shahr A Alshahr
Electrical Engineering Department
Western Michigan University
Kalamazoo, MI 49008. USA
Shahrabdulkrai.Alshahr@wmich.edu

2nd Bilal Eid
Department of Electrical-Electronic Engineering
Hasan Kalyoncu University
Gaziantep, Turkey
bilal.eid@hku.edu.tr

3rd Johnson A Asumadu
Electrical Engineering Department
Western Michigan University
Kalamazoo, MI 49008. USA
johnson.asumadu@wmich.edu

***Abstract*—This paper discusses active and reactive power controlling techniques in microgrids and categorizes them based on complexity levels and purposes. The three main investigated techniques in this paper are; reactive power injection, reactive power at night and power curtailment. Additionally, it explains the profitability of these aspects to the investors and recommends modifications and improvements to enhance microgrid and power grid integration.**

***Index Terms*—Distributed energy resources, controlling models, Microgrid.**

I. Introduction

At first glance, the idea of assessing the profitability of a microgrid may seem simple, the cost of the microgrid and how much energy is saved by the customer. However the saving in the energy bills is not only the value of microgrids, but microgrids provide value in several ways not directly reflected in the cost of energy. Energy reliability is one of the most important, and the most difficult value to achieve. Keeping the power flowing when the main grid is off often the main reason why customers choose to install microgrids [1]–[3]. So the critical question here is: What is the cost of a power outage. The answer varies from customer to customer. The other significant value for microgrid is the ability to contribute to the stability of the power system responding to the load, regulation the voltage and frequency. The value of these ancillary services varies from country to country and has no straight forward computational technique.

In order to maximize the value of the microgrids, the microgrid's controller and power management techniques have to be implemented professionally. The major expenses of the microgrid are; DER assets, grid automation, microgrid optimization software, development, and installation costs, and energy storage. Figure 1 represents the cost of microgrid controller and represents 15 percent of the overall development costs. However, the key differentiator between the smart, optimized microgrid and simple control projects such as a PV solar project with a battery, is the controller. The microgrid controller is the main value that enables the technical islanding functionality when needed [4], [5]

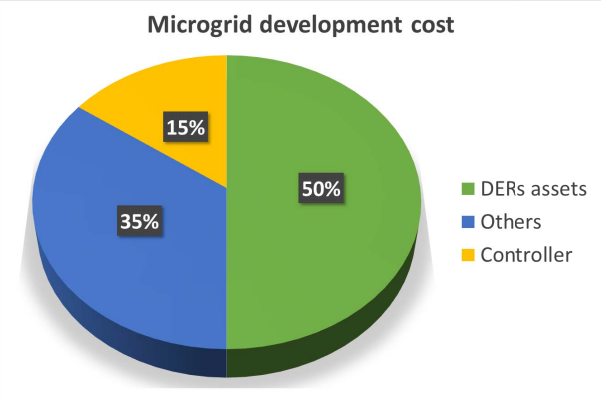

Fig. 1. Microgrid development cost

The organization of this paper is as follows: Section II describes the microgrid's levels of controlling. Section III describes the microgrid controller modeling. Sections IV presents the controlling classifications and improvements,and Section V concludes the paper.

II. Microgrid's levels of controlling

It is not necessary to build the microgrids at once,but be extended and improved in phases, with additional sophistication and capabilities integrated over time. By taking this approach, a continuous investment can be taken by the customers, gaining confidence as the microgrid proves its feasibility. The correct start is to start from the existing infrastructure, both on-site and on the grid. Once the existing infrastructure has been used effectively, the project can begin to improve the microgrid capabilities, starting with the primary goals of the customers or supplying the critical loads.

Six different levels of control can be identified with microgrid, stepping up from the simplest, which has only a back-up generator to the most advanced microgrid with multiple DERs, energy storage devices, advanced controller capabilities, and

978-1-7281-5317-9/20/$31.00 ©2020 IEEE

even the top ability to coordinate multiple microgrids.(See Fig. 2). For any customer, electric reliability is usually the priority. Because of this, the first phase of improvement might be to isolate a circuit and add controllers so that the existing DER can stay up and running in stand-alone mode of operation as shown in level one in Fig. 2. Once the microgrid is established to provide the customers with reliability, integration of one or more DERs can operate in both mode of operations grid-connected and stand-alone. In level two, the Microgrid and also participate in day-ahead (DA) energy market.

Different electrical and thermal assets can be included in every microgrid, such as combined heat and power (CHP) systems, diesel generators or natural gas, PV systems with or without batteries, boilers, and chillers. The thermal and electrical networks will be supported by these assets to generate the required heat and electricity [6], [7]. Thermal and battery storage assets will be seamlessly integrated and managed in the controller of level three. In level three , the aim is to maintain the full system availability and optimizition the lifetime of existing thermal assets. In level four, the whole controlling capability of level three is there plus the load management capability.

At optimization of level five, it is important to use the resources for the best economics. For instant, adding controllers that support existing microgrid DERs to provide; frequency support, peak load shaving, load time-shifting, or ancillary services to the grid. In order to achieve these ancillary services at this level, the microgrid should be capable of forecasting the weather, the generation, and achieving economic dispatch. presently, the highest controlling level of a microgrid in operation is level five, as shown in Fig. 2. The highest microgrid in planning is a Level six, which opens the door for a distribution network where multi-microgrids interact with each other and share resources. The development of the controller at this level is now under process ongoing by many companies and researchers [8].

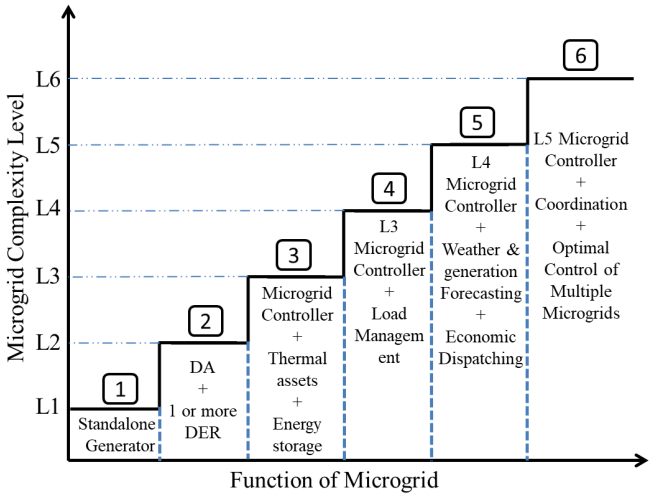

Fig. 2. Microgrid controlling levels of complexity

III. Microgrid Controller Modeling

In any electronically coupled DERs the inverter is the main controlling part of the controlled circuit. It is essential to have clear derivation for the the three-phase inverters used in the microgrid. Figure 3 showes 3 show the three-phase inverter connected to the grid. The controlling block (in dashed blue) of the three phase inverter is shown in Fig. 3. The inputs are the I_{abc}, V_{abc} and V_{dc} which are measured values.

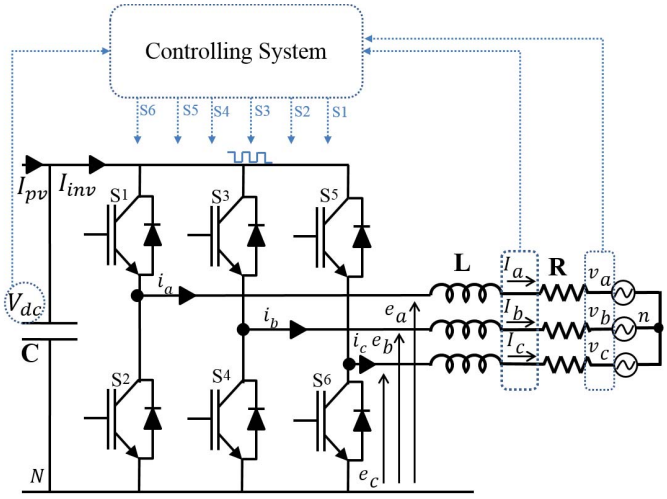

Fig. 3. Three phase inverter connected to the grid

The controlling stages inside the controlling system are shown in Fig. 4. There are 5 blocks performing the following functions; Phase locked loop (PLL), converting abc three phase reference frame to dq0 rotating reference frame, regulating voltage, regulating current, and the controller for reactive power and generation of pulses.

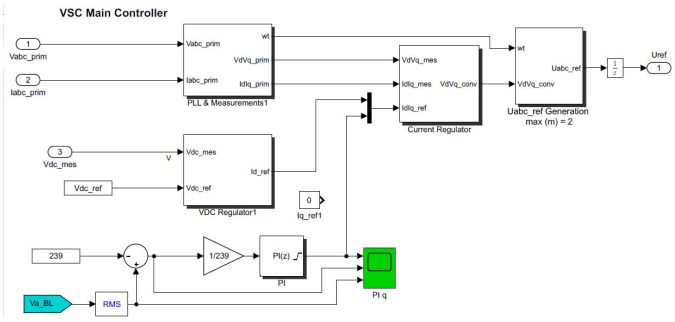

Fig. 4. The controlling system of the inverter

Converting abc three phase reference frame to dq0 rotating reference frame, is an essential simplification stage in controlling the system. This stage is shown in Fig. 5. In this stage PLL is so important to maintain the phase of the grid. The park transformation is used to convert abc to dq0 reference frame.

To achieve proper modeling for the three phase inverter shown in Fig. 3, the assumption of symmetrical and sinusoidal three phase voltage is adopted and shown in (1):

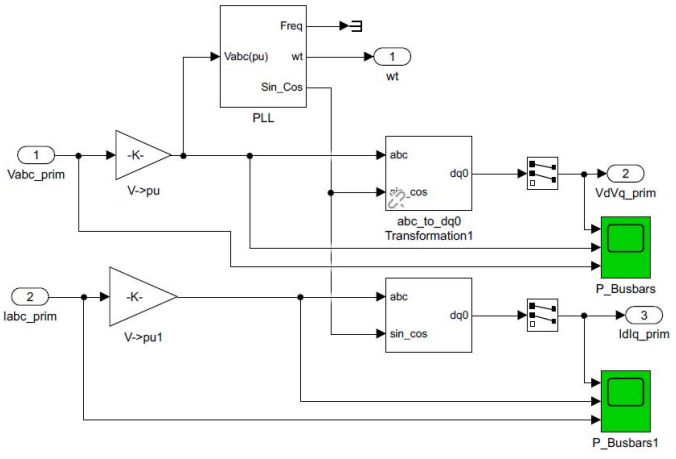

Fig. 5. abc three phase reference frame to dq0 rotating reference frame transformation block

$$\left\{\begin{array}{c} v_a = V_m cos(wt) \\ v_b = V_m cos(wt - \frac{2}{3}\pi) \\ v_c = V_m cos(wt + \frac{2}{3}\pi) \end{array}\right\} \quad (1)$$

where V_m is the voltage's peak value. The inverter model in the abc reference frame is derived and the output voltage is shown in fig.3, and the input DC voltage equations are shown in [2]

$$\left\{\begin{array}{c} e_a = L\frac{di_a}{dt} + i_a R + v_a + v_{nN} \\ e_b = L\frac{di_b}{dt} + i_b R + v_b + v_{nN} \\ e_c = L\frac{di_c}{dt} + i_c R + v_c + v_{nN} \\ I_{pv} = C\frac{dv_{dc}}{dt} + I_{inv} \end{array}\right\} \quad (2)$$

Figure 3 showes the resistor R and capacitor C. The voltage to ground is from (3) as

$$v_{nN} = \frac{1}{3}(e_a + e_b + e_c) \quad (3)$$

The inverter's switching function $d_k^*(k = 1, 3, 5)$ is defined as shown in (4) (where d_k^* is the switching function of the switching device S_k, k is the number of switches as shown in Figure [3]. The switches in the same phase must not has the same switching position at the same time.

$$d_k^* = \left\{\begin{array}{l} 1, \ \ if\ S_k\ is\ on\ and\ S_{k+1}\ is\ \ off \\ 0, \ \ if\ S_k\ is\ off\ and\ S_{k+1}\ is\ \ on \end{array}\right\} \quad (4)$$

From (4) when the S_k is on, d_k^* = 1 otherwise, d_k^*=0, Moreover if the switch number 1 (S_1) is on the switch number 2 (S_2) is off, phase a will not be in short circuit mode at anytime. The voltage values per phase are calculated based on switch position at that period from (5) below:

$$e_a - v_{nN} = V_{dc}(d_1^* - \frac{d_1^* + d_3^* + d_5^*}{3}) \quad (5)$$

Equation (5) is for phase a and for phases b and c only d_1^* will be change to d_3^* and d_5^* respectively. Also I_{inv} can be calculated from (6) below:

$$I_{inv} = d_1^* i_a + d_3^* i_b + d_5^* i_c \quad (6)$$

Therefore, the model (2) can be written as in equation (7) below:

$$\left\{\begin{array}{c} L\frac{di_a}{dt} = -i_a R - v_a + (d_1^* - \frac{d_1^*+d_3^*+d_5^*}{3})v_{dc} \\ L\frac{di_b}{dt} = -i_b R - v_b + (d_3^* - \frac{d_1^*+d_3^*+d_5^*}{3})v_{dc} \\ L\frac{di_c}{dt} = -i_a R - v_c + (d_5^* - \frac{d_1^*+d_3^*+d_5^*}{3})v_{dc} \\ C\frac{dv_{dc}}{dt} = I_{pv} - (d_1^* i_a + d_3^* i_b + d_5^* i_c) \end{array}\right\} \quad (7)$$

From (7), the model can be converted to matrix formula as shown in (8)

$$\begin{bmatrix} \frac{di_a}{dt} \\ \frac{di_b}{dt} \\ \frac{di_c}{dt} \\ \frac{dv_{dc}}{dt} \end{bmatrix} = \begin{bmatrix} -\frac{R}{L} & 0 & 0 & \frac{d_1}{L} \\ 0 & -\frac{R}{L} & 0 & \frac{d_2}{L} \\ 0 & 0 & -\frac{R}{L} & \frac{d_3}{L} \\ -\frac{d_1^*}{C} & -\frac{d_2^*}{C} & -\frac{d_3^*}{C} & 0 \end{bmatrix} \begin{bmatrix} i_a \\ i_b \\ i_c \\ v_{dc} \end{bmatrix} + \begin{bmatrix} -\frac{1}{L} & 0 & 0 & 0 \\ 0 & -\frac{1}{L} & 0 & 0 \\ 0 & 0 & -\frac{1}{L} & 0 \\ 0 & 0 & 0 & \frac{1}{C} \end{bmatrix} \begin{bmatrix} v_a \\ v_b \\ v_c \\ I_{pv} \end{bmatrix} \quad (8)$$

From fourier analysis the PWM inputs in (7) can be separated into high-frequency and low-frequency components following Fourier analysis. The low-frequency component is the same as (7), with the switching functions d^* being replaced by continuous duty ratios $d_k^*(k = 1, 3, 5)$, containing 2 states $\in [0, 1]$ as shown in [9]. in[10], ([9]is used for the conversion of the dq references) is used to generate(1).

$$T_{dq0}^{abc} = \begin{bmatrix} 0 & -w & 0 \\ w & 0 & 0 \\ 0 & 0 & 0 \end{bmatrix} \quad (9)$$

$$\begin{bmatrix} \frac{di_d}{dt} \\ \frac{di_q}{dt} \\ \frac{di_0}{dt} \\ \frac{dv_{dc}}{dt} \end{bmatrix} = \begin{bmatrix} -\frac{R}{L} & \omega & \frac{d_d}{L} \\ -\omega & -\frac{R}{L} & \frac{d_q}{L} \\ 0 & 0 & 0 \\ -\frac{d_d}{C} & -\frac{d_q}{C} & 0 \end{bmatrix} \begin{bmatrix} i_d \\ i_q \\ v_{dc} \end{bmatrix} + \begin{bmatrix} -\frac{1}{L} & 0 & 0 \\ 0 & -\frac{1}{L} & 0 \\ 0 & 0 & 0 \\ 0 & 0 & \frac{1}{C} \end{bmatrix} \begin{bmatrix} v_d \\ v_q \\ I_{pv} \end{bmatrix} \quad (10)$$

By removing the 0 sequence the whole dynamic model is (11):

$$\begin{bmatrix} \frac{di_d}{dt} \\ \frac{di_q}{dt} \\ \frac{dv_{dc}}{dt} \end{bmatrix} = \begin{bmatrix} -\frac{R}{L} & \omega & \frac{d_d}{L} \\ -\omega & -\frac{R}{L} & \frac{d_q}{L} \\ -\frac{d_d}{C} & -\frac{d_q}{C} & 0 \end{bmatrix} \begin{bmatrix} i_d \\ i_q \\ v_{dc} \end{bmatrix} + \begin{bmatrix} -\frac{1}{L} & 0 & 0 \\ 0 & -\frac{1}{L} & 0 \\ 0 & 0 & \frac{1}{C} \end{bmatrix} \begin{bmatrix} v_d \\ v_q \\ I_{pv} \end{bmatrix} \quad (11)$$

where: i_d is d axis grid currents, i_q is q axis grid currents, v_d is d axis grid voltages, v_q is q axis grid voltages, d_d is d axis duty ratios, d_q is q axis duty ratios. Model (11) is the required variation in i_d and i_q.

Model expressed by (11) shows that there is a cross-coupling between the d and q components, which affects the dynamic performance of the regulator [10]. Therefore, for better performance, decoupling th two axes is necessary, which can be accomplished by feed-forward decoupling control method. Assuming:

$$\left\{\begin{array}{l} \nu_{rd} = -V_d + d_d V_{dc} + \omega L i_q \\ \nu_{rq} = -V_q + d_q V_{dc} + \omega L i_d \end{array}\right\} \quad (12)$$

Then from the model given by (11), the system expressions become

$$\left\{\begin{array}{c} \frac{di_d}{dt} = -\frac{R}{L}i_d + \frac{1}{L}\nu_{rd} \\ \frac{di_q}{dt} = -\frac{R}{L}i_q + \frac{1}{L}\nu_{rq} \\ \frac{dv_{dc}}{dt} = \frac{I_{pv}}{C} - \frac{V_d+\nu_{rd}}{CV_{dc}}i_d - \frac{V_q+\nu_{rq}}{CV_{dc}}i_q \end{array}\right\} \quad (13)$$

Model (13) eliminates the cross-coupling variables. Therefore, the currents i_d and i_q can be controlled independently by acting upon inputs V_d and V_q, respectively. Controlling i_q leads to regulating the reactive power whereas controlling i_d can be used fro active power curtailment. Section IV explains these two controllers.

IV. Controlling Classifications and Improvements

To fully optimize the microgrid many parameters have to be considered. . The parameters include current electricity cost, hourly electricity prices at any given time, fuel savings derived from CHP, and availability of controllable loads (that can affect the effect of load shifting on utility charges). Additional parameters are change over time for load profile, size and efficiency of DERs, and fuel cost [11]–[14]. The controllers of the microgrid are classified into two main controllers; one for reactive power and the other for active power.

A. Controlling Reactive power

The reactive power can be controlled via the inverter by regulating the current. One of the important strategies is to measure the voltage and regulate the reactive power accordingly. figure. 6 explains one of the main reactive power controlling strategy. If the grid voltage (V_g) is higher than 0.9 of normal grid voltage (V_{gn}), the system will follow the initial condition of active current (i_dn). If V_g is in between 0.9 V_{gn} and 0.3 V_{gn}, the controlling algorithm should act to regulate the i^*_{dnew}. If V_g is less than 0.3 V_{gn} (normally for severe grid fault), no i_d should be delivered to the system to avoid more power losses. The flowchart of the above process is shown in Fig. 6

Reactive Power at night:One of the recent features of PV power plant is reactive power at night, when the PV plant can inject/absorb reactive power at night to contribute to the grid stability [15]–[17]. Reactive power at night option in the modern inverters include additional hardware components that enable operation even without the availability of the DC source.

The function of reactive power at night is to provide PV power plant operators with extra advantages. First of all, it meets the reactive power needs of their PV power plant and supplies power to any installed local electrical appliances, eliminating the need to purchase reactive power or the expenses for a compensation plant. Moreover, a further revenue can be generated by supplying additional reactive power once required by the grid operators [15]–[17].

B. Controlling Active Power

Frequency control is essential for each power system to mitigate the instability issues. In order to achieve this active power curtailment can be implemented. Active power curtailment can be used to control the frequency by reducing up to 40% of the generated active power in order to contribute to grid stability. Irradiation and temperature variations also have a great impact on the PV output, which result in power fluctuations leading to changes in frequency and system instability [18]. The control of active power is achieved via the inverter controlling i_d which will increase the profitability of the microgrid.

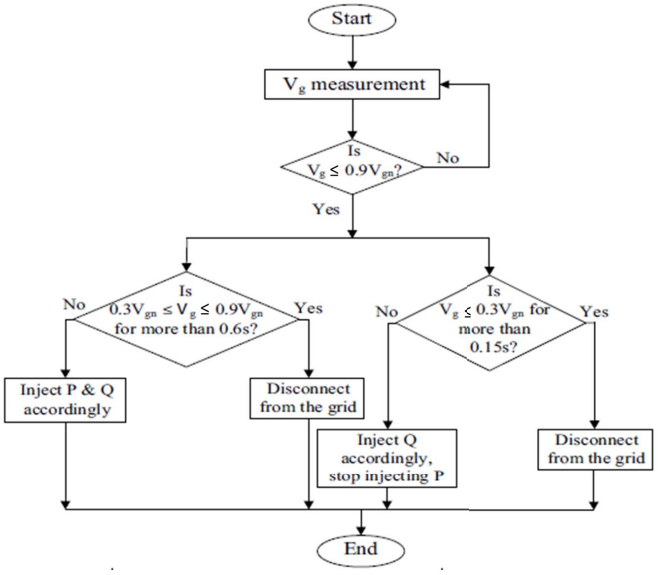

Fig. 6. Proposed modification for the voltage regulation strategy

V. Conclusions

In microgrids, controllers regulate active and reactive power to create a balance that stabilizes the distribution network as well as allows maximum power for them. In this paper, the main control techniques in microgrids have been discussed. The paper has classified controlling techniques based on their main functions; reactive power injection, reactive power at night and power curtailment. Various derivations of control models has been demonstrated, which showed that currents and voltages constitute inputs of the controlling blocks while the outputs are pulses that control the switches. Some modifications to control reactive power have been proposed in order to enhance voltage profile and system stability.

Also discussed is the importance of using advanced microgrid controllers to optimize the DERs and its profitability and return on investment for microgrid projects. In this study, the controlling system accounts for only 15 percent of the microgrid development cost yet the controlling system is largely responsible for system's profitability increase. However, to better understand economic value and profitability of controllers, the price for power resiliency and maintaining power supply during grid power outages need to be studied.

ACKNOWLEDGMENT

The authors thank Hasan Kalyoncu University and Western Michigan University for the technical assistance received.

REFERENCES

[1] E. A. M. Ceseña, N. Good, A. L. Syrri, and P. Mancarella, "Techno-economic and business case assessment of multi-energy microgrids with co-optimization of energy, reserve and reliability services," *Applied energy*, vol. 210, pp. 896–913, 2018.

[2] T. Adefarati and R. Bansal, "Reliability, economic and environmental analysis of a microgrid system in the presence of renewable energy resources," *Applied Energy*, vol. 236, pp. 1089–1114, 2019.

[3] M. Stadler, G. Cardoso, S. Mashayekh, T. Forget, N. DeForest, A. Agarwal, and A. Schönbein, "Value streams in microgrids: A literature review," *Applied Energy*, vol. 162, pp. 980–989, 2016.

[4] P. Singh, "Technical and economic potential of microgrids in california," 2017.

[5] A. Khamis, Y. Xu, Z. Y. Dong, and R. Zhang, "Faster detection of microgrid islanding events using an adaptive ensemble classifier," *IEEE Transactions on Smart Grid*, vol. 9, no. 3, pp. 1889–1899, 2018.

[6] S. D. Nazemi, K. Mahani, A. Ghofrani, B. Ece Köse, and M. Jafari, "Techno-economic analysis and optimization of a microgrid considering demand-side management," in *Proceedings of the 2019 Institute of Industrial and Systems Engineers (IISE) Annual Conference*, 04 2019.

[7] S. Tsianikas, J. Zhou, N. Yousefi, and D. W. Coit, "Battery selection for optimal grid-outage resilient photovoltaic and battery systems," *arXiv preprint arXiv:1901.11389*, 2019.

[8] H. Wang and J. Huang, "Incentivizing energy trading for interconnected microgrids," *IEEE Transactions on Smart Grid*, vol. 9, no. 4, pp. 2647–2657, 2018.

[9] R. Wu, S. B. Dewan, and G. R. Slemon, "Analysis of an ac-to-dc voltage source converter using pwm with phase and amplitude control," *Industry Applications, IEEE Transactions on*, vol. 27, no. 2, pp. 355–364, 1991.

[10] R. Kadri, J.-P. Gaubert, and G. Champenois, "An improved maximum power point tracking for photovoltaic grid-connected inverter based on voltage-oriented control," *Industrial Electronics, IEEE Transactions on*, vol. 58, no. 1, pp. 66–75, 2011.

[11] Z. Bo, Z. Xuesong, and C. Jian, "Integrated microgrid laboratory system," *Power Systems, IEEE Transactions on*, vol. 27, no. 4, pp. 2175–2185, 2012.

[12] Z. Chen, "A review of power electronics based microgrids," *Journal of Power Electronics*, vol. 12, no. 1, 2012.

[13] M. Savaghebi, A. Jalilian, J. C. Vasquez, and J. M. Guerrero, "Autonomous voltage unbalance compensation in an islanded droop-controlled microgrid," *Ieee Transactions on Industrial Electronics*, vol. 60, no. 4, 2013.

[14] W. Du, Q. Jiang, M. Erickson, and R. Lasseter, "Voltage-source control of pv inverter in a certs microgrid," *Power Delivery, IEEE Transactions on*, vol. 29, no. 4, pp. 1726–1734, Aug 2014.

[15] N. Solanki and J. Patel, "Utilization of pv solar farm for grid voltage regulation during night; analysis & control," in *2016 IEEE 1st International Conference on Power Electronics, Intelligent Control and Energy Systems (ICPEICES)*. IEEE, 2016, pp. 1–5.

[16] R. K. Varma, S. A. Rahman, and T. Vanderheide, "New control of pv solar farm as statcom (pv-statcom) for increasing grid power transmission limits during night and day," *IEEE transactions on power delivery*, vol. 30, no. 2, pp. 755–763, 2015.

[17] M. A. Bhaskar, B. Vidya, S. Dash, C. Subramani, and M. J. Kumar, "Application of integrated wind energy conversion system (wecs) and photovoltaic (pv) solar farm as statcom to regulate grid voltage during night time," in *India International Conference on Power Electronics 2010 (IICPE2010)*. IEEE, 2011, pp. 1–6.

[18] H. Xin, Y. Liu, Z. Wang, D. Gan, and T. Yang, "A new frequency regulation strategy for photovoltaic systems without energy storage," *IEEE Transactions on Sustainable Energy*, vol. 4, no. 4, pp. 985–993, 2013.